Developmental Biology **214,** 168–180 (1999)
Article ID dbio.1999.9396, available online at http://www.idealibrary.com on IDEAL®

Zebrafish Eggs on Activation

Karen W. Lee, Sarah E. Webb, and Andrew L. Miller[1]

Department of Biology, HKUST, Clear Water Bay, Kowloon, Hong Kong SAR, People's Republic of China

The activation process in a variety of deuterostome and protostome eggs is accompanied by cytosolic calcium transients that usually take the form of either a single or multiple propagating waves. Here we report that the eggs of zebrafish (*Danio rerio*) are no exception in that they generate a single activation wave that traverses the egg at a velocity of around 9 μm/s. There appears, however, to be no difference between the calcium-mediated activation response of eggs with regard to the presence or absence of sperm in the spawning medium. This leads us to suggest that these eggs are normally activated when they come in contact with their spawning medium and are then subsequently fertilized. The aspermic wave is initiated at the animal pole in the region of the micropyle, appears to propagate mainly through the yolk-free egg cortex, and then terminates at the vegetal pole. As neither sperm nor external calcium is required for the initiation (or propagation) of the activation wave, this suggests that an alternative wave trigger must be involved.

Key Words: **calcium; aequorin; zebrafish; activation; fertilization.**

INTRODUCTION

It appears that all vertebrate, invertebrate, and perhaps even some plant eggs are activated by the generation of calcium transients in their cytoplasm (Roberts *et al.*, 1994; Shen, 1995; Digonnet *et al.*, 1997; Lawrence *et al.*, 1997). In most cases, apart from a recent report on the marine worm *Urechis caupo* (Stephano and Gould, 1997), these transients take the form of propagating calcium waves (Galione *et al.*, 1993; Jaffe, 1993), which appear to provide a significant component of the activating stimulus required for these eggs (Jaffe, 1985; Epel, 1990; Whitaker and Swann, 1993). It is becoming clear, however, that although wave propagation is a common feature of activation, there are both subtle and significant differences in this response when comparing eggs from different species. For example, in fish (Gilkey *et al.*, 1978; Yoshimoto *et al.*, 1986), echinoderms (Steinhardt *et al.*, 1977; Stricker *et al.*, 1992; Gillot and Whitaker, 1993), and frogs (Busa and Nuccitelli, 1985; Kubota *et al.*, 1987), a single calcium wave is propagated across the activating egg. In contrast, activation triggers a series of repetitive calcium waves or oscillations in annelids (Eckberg and Miller, 1995; Stricker, 1996), ascidians (Speksnijder *et al.*, 1990; Albrieux *et al.*, 1997), and mammals (Miyazaki *et al.*, 1986, 1993; Kline and Kline, 1992; Swann, 1994; Miyazaki, 1995), including humans (Homa and Swann, 1994; Tesarik and Testart, 1994).

With regard to the role of calcium in the activation of fish eggs, most of our information derives from work on the medaka, *Oryzias latipes* (Gilkey *et al.*, 1978; Yoshimoto *et al.*, 1986; Iwamatsu *et al.*, 1988). Teleost eggs, however, display a remarkable variety of adaptations. We decided, therefore, to examine the calcium-related activation/fertilization response in the egg of the zebrafish (*Danio rerio*), as it has significant differences in morphology, activation/fertilization strategy, and cortical granule (CG) reaction compared to the medaka (Hart, 1990). Furthermore, the resurgent interest in understanding zebrafish embryology as a model system for vertebrate development (Kimmel *et al.*, 1995) made it a very appropriate candidate for this comparative study.

Morphologically, mature zebrafish eggs differ significantly from those of medaka. While the latter possess a central yolk mass, separated from the peripheral cytoplasm by a continuous yolk membrane (Gilkey *et al.*, 1978), zebrafish eggs possess many individual membrane-bound yolk globules that are homogeneously intermingled with ooplasm throughout the mature oocyte (Beams *et al.*, 1985). However, although not structurally separated by a continu-

[1] To whom correspondence should be addressed. Fax: (852) 2358 1559. E-mail: almiller@ust.hk.

0012-1606/99 $30.00

ous membrane, these eggs do possess a functional ooplasmic cortex some 15–20 μm thick where yolk globules are excluded. This oocyte cortex contains a network of endoplasmic reticulum (ER), filamentous actin, and an array of CGs (Hart, 1990). The CGs are arranged in multiple layers, which is quite unlike the situation found in medaka, where they form a single layer just beneath the plasma membrane (Hart and Yu, 1980).

Histological studies have shown that ovulation and oviposition in zebrafish occur only when they mate; i.e., eggs are not present in the ovarian lumen nor in the oviduct of females even when they are kept together with males. This indicates that the egg is normally retained within the ovarian stroma except when the fish breed (Hisaoka and Firlit, 1962). When mature zebrafish eggs are discharged from the ovarian stroma and come in contact with the spawning medium, they activate (Hart and Yu, 1980; Hart and Fluck, 1995; Sakai *et al.*, 1997). Even in the absence of sperm, these activated eggs undergo a programmed series of developmental steps. Initially there is an almost instantaneous reduction in egg size due to the contraction of the egg surface (Roosen-Runge, 1938; Hart and Yu, 1980). This results in an initial small separation of the chorion from the plasma membrane. Within 30 s after the onset of activation, the CG reaction is initiated and occurs more or less simultaneously over the entire surface of the egg. These parthenogenetically activated eggs then proceed to elevate their chorions and undergo normal ooplasmic segregation. After several abortive cleavages, however, they fail to develop further. If sperm are present in the spawning medium, an identical series of steps is observed but cell division is normal and development proceeds.

Medaka eggs on the other hand do not display such activation on contact with their spawning medium, although they do become "less fertilizable" the longer they remain in the absence of sperm (Yamamoto, 1944, 1961). On activation, either by sperm or via a parthenogenetic means such as application of the ionophore A23187 (Gilkey *et al.*, 1978) or digitalin, for example (Yamamoto, 1961), a wave of calcium-induced calcium release (CICR) sweeps through the cytoplasm of the medaka egg at a velocity of around 13 μm/s (Gilkey *et al.*, 1978). This wave originates at the site of either sperm entry or parthenogenetic stimulation and is considered to represent Yamamoto's invisible "fertilization wave" (Yamamoto, 1944). The calcium wave in medaka is followed some 17 s later by a wave of CG fusion that results in the elevation of the chorion (Yoshimoto *et al.*, 1986).

Thus, as the morphology, activation/fertilization strategy, and CG reaction in zebrafish are clearly different than those described in medaka, we wished to explore whether the activation of zebrafish eggs involved the generation of a typical fast calcium activation wave (Jaffe, 1993) and, if so, to determine the relationship between this and the other morphological steps in the activation process.

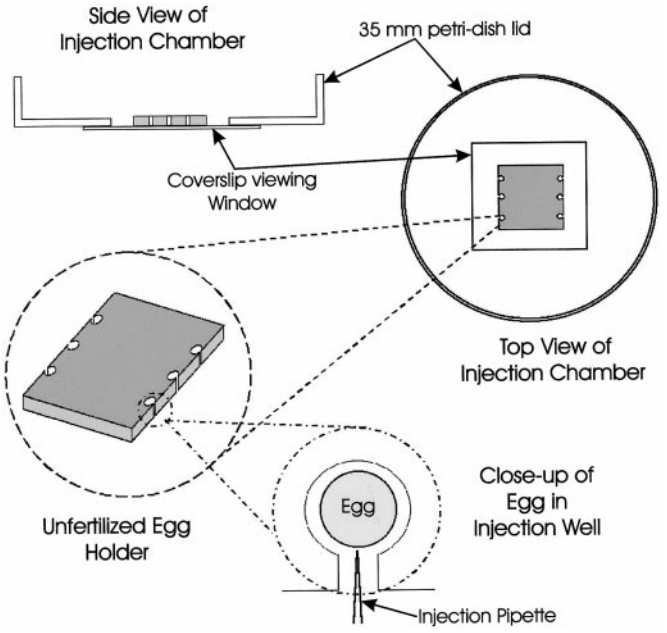

FIG. 1. Schematic outline of our custom-designed egg injection chamber.

MATERIALS AND METHODS

Egg Collection

Zebrafish (*D. rerio*) were maintained on a 14-h light/10-h dark cycle to stimulate spawning (Westerfield, 1994). Unactivated eggs and sperm were squeezed directly from fish by methods modified from Westerfield (1994). Unactivated eggs were collected using 50-μl micropipettes (Wiretrol; Drummond Scientific Co.) prewetted with either coho salmon ovarian fluid (SOF; Corley-Smith *et al.*, 1996; SeaTech Bioproducts) or 0.5% bovine serum albumin (BSA fraction V; Sigma) in Hank's buffered saline (0.137 M NaCl, 5.4 mM KCl, 0.25 mM Na_2HPO_4, 1.3 mM $CaCl_2$, 1.0 mM $MgSO_4$, 4.2 mM $NaHCO_3$) and placed in a custom-designed injection chamber in either SOF or BSA solution (Fig. 1). Sperm were collected using a 50-μl micropipette prewetted with sperm extender solution (10 mM Hepes, 80 mM KCl, 45 mM NaCl, 45 mM $C_2H_3NaO_2$, 0.4 mM $CaCl_2$, 0.2 mM $MgCl_2$) and stored in sperm extender solution on ice until required.

Microinjection Procedures

As unactivated zebrafish eggs are difficult to microinject, during both the penetration and the withdrawal of the micropipette, an injection chamber was designed to overcome these problems. The chamber consisted of a 12 × 10 × 1 mm Plexiglas block into which holes of 800-μm diameter were cut. The holes were set approximately 1 mm away from the edge of the block, but were open to the edge via a 200-μm-wide side slit that extended downward for the entire depth of the hole. The block was mounted on a coverglass (22 × 22 mm; No.1) using a small amount of high-vacuum silicone grease (Dow Corning Corp.) and then the coverglass itself was

attached (also with silicone grease) underneath a hole cut in a 35-mm petri dish lid. Unactivated eggs were placed in the holes on the Plexiglas block and microinjected through the side slit. The design of the chamber prevented both excess rotation during penetration of the micropipette and the egg from sticking to the tip of the micropipette when it was withdrawn following injection (see Fig. 1). Eggs were also activated and fertilized while held in these chambers, which provided reasonable inverted viewing optics for imaging. The injection chambers prevented full elevation of the egg chorion, however, this did not have any effect on subsequent early development (see Fig. 4L).

Microinjection of Aequorins

The microinjection pipettes and the pressure injection system used for injecting unfertilized eggs are described in detail elsewhere (Webb *et al.*, 1997). All glassware and plasticware associated with the aequorin injections were prewashed for several minutes with 100 μM EGTA. Micropipettes were front-filled and washed with EGTA prior to being filled with aequorin. Approximately 3.0 nl of recombinant *f*- or *h*-aequorin (1% in 100 mM KCl, 5 mM Mops, and 50 μM EDTA; Shimomura *et al.*, 1990) was injected into the center of unfertilized eggs. Following injection, eggs were transferred to our photon imaging microscope (PIM; Science Wares) or a photomultiplier tube (PMT; H5920-01; Hamamatsu) for data acquisition. The aequorin was allowed time to diffuse evenly throughout the egg (a process that took approximately 20 min) before eggs were activated. During this time a resting level of luminescence was obtained for each experiment.

Egg Activation/Fertilization

In order to either activate eggs in the absence of sperm or to activate and fertilize eggs in the presence of sperm, data acquisition was briefly suspended, and the 0.5% BSA in Hank's buffered saline, or SOF, was removed from the injection well. In the case of activation in the absence of sperm, 100 μl of 0.5% fructose in egg-water (60 μg/ml "Instant Ocean" in deionized water) was added to the well. In the case of activation followed by fertilization, 30 μl of concentrated sperm suspension (in sperm extender solution) was placed in the well. Allowing approximately 30 s for the sperm to drop to the level of the egg, 100 μl of 0.5% fructose in egg-water was then added to the injection chamber to activate the sperm. Data acquisition was then immediately resumed.

Aequorin-Derived Data Acquisition and Review

Photon imaging. Aequorin-generated images were gathered using our custom-designed PIM. A simplified schematic outline of this system is shown in Fig. 2A (for details see Webb *et al.*, 1997). Both bright-field and photon images were collected using either a Zeiss Plan Neofluar 10×/0.3 NA or 5×/0.15 NA objectives. Our system allows us to review aequorin-generated photon data with any chosen integration periods and time steps. In addition, we can correlate photon events with morphological features by superimposing the photon data on intermittently captured bright-field images. The photon and corresponding bright-field images were exported in. TIFF file format to Metamorph 3.0 (Universal Imaging) for detailed quantitative data analysis and downloaded into Corel Photo Paint 7 and Corel Draw 7 (Corel Corp.) for figure preparation and presentation.

Photon counting. Quantitative aequorin-generated data were also acquired using our PMT system, which is outlined in Fig. 2B. The system has been designed so as to place the aequorin-loaded egg (within the injection/viewing chamber, see Fig. 1) as close to the bialkali photocathode as possible. A 25-mm-diameter Uniblitz VS electronic shutter is positioned directly above the photocathode in order to protect it from ambient light during sample manipulation. During data collection, the injection chamber is covered with a concave reflective mirror to direct light onto the photocathode surface. In addition, the whole system is mounted within a dark box to block ambient light from the photocathode when it is exposed to light from the sample. The output pulses from the PMT are recorded by a computerized data acquisition system, called PMT for Windows 95 (Science Wares), via an electronic interface unit. This software stores the count rate values in a sequential file and allows data acquisition parameters and text comments from an experimental log to be recorded on a separate file. The program provides real-time and postexperimental data displays as well as a variety of analysis functions. PMT-generated data were downloaded into Microsoft Excel 97 for graph plotting.

Microinjection of Fluorescent Microspheres

Any rotational movements of eggs during the activation process (i.e., once the plasma membrane and chorion separate) would greatly increase the complexity of analyzing our imaging data. Thus, experiments were carried out to check for egg rotation during activation. Approximately 2.3 nl of a 0.1% suspension of Nile red microspheres (2 μm; carboxylate-modified; dissolved in 150 mM KCl, 5 mM Hepes, pH 7.0; Molecular Probes) was injected into the periphery of eggs, approximately 50 μm below the plasma membrane. Injected eggs were then transferred to a Bio-Rad MRC-600 laser scanning confocal imaging system equipped with a krypton/argon mixed gas laser, mounted on an upright microscope (Axioskop; Zeiss). Both bright-field and fluorescent images were collected using a Zeiss Plan Neofluar 10×/0.3 NA objective. The most appropriate optical plane containing the fluorescent microspheres was located, and the eggs were then activated using 0.5% fructose in egg-water (as described earlier). A confocal time-series (every 15 s) of microsphere-loaded eggs was then recorded.

We reviewed the corresponding fluorescent and bright-field images using Confocal Assistant 4.02 (downloaded from the Bio-Rad FTP server: ftp://ftp.genetics.biorad.com/public/confocal in .PIC file format) and Metamorph 3.0. Presentation files for figure preparation were downloaded into Corel Photo Paint 7 and Corel Draw 7.

Calcium-Free Experiments

In a series of experiments, stringent precautions were taken to ensure that calcium-free conditions were created and maintained external to unactivated eggs, before and during the activation process. Calcium-free 0.5% BSA in Hank's buffered saline solution was prepared in ultrapure deionized H_2O by omitting $CaCl_2$ and adding 0.3 mM EGTA to chelate trace levels of contaminating calcium arising from the other components. All glassware and plasticware used in handling eggs were also prewashed for several minutes with 100 μM EGTA solution. Unactivated eggs were collected (as described above) in calcium-free 0.5% BSA in Hank's buffered saline.

Video Recording Egg Activation

Real-time video recordings of the activation process both in the presence and in the absence of sperm were made using a CCD

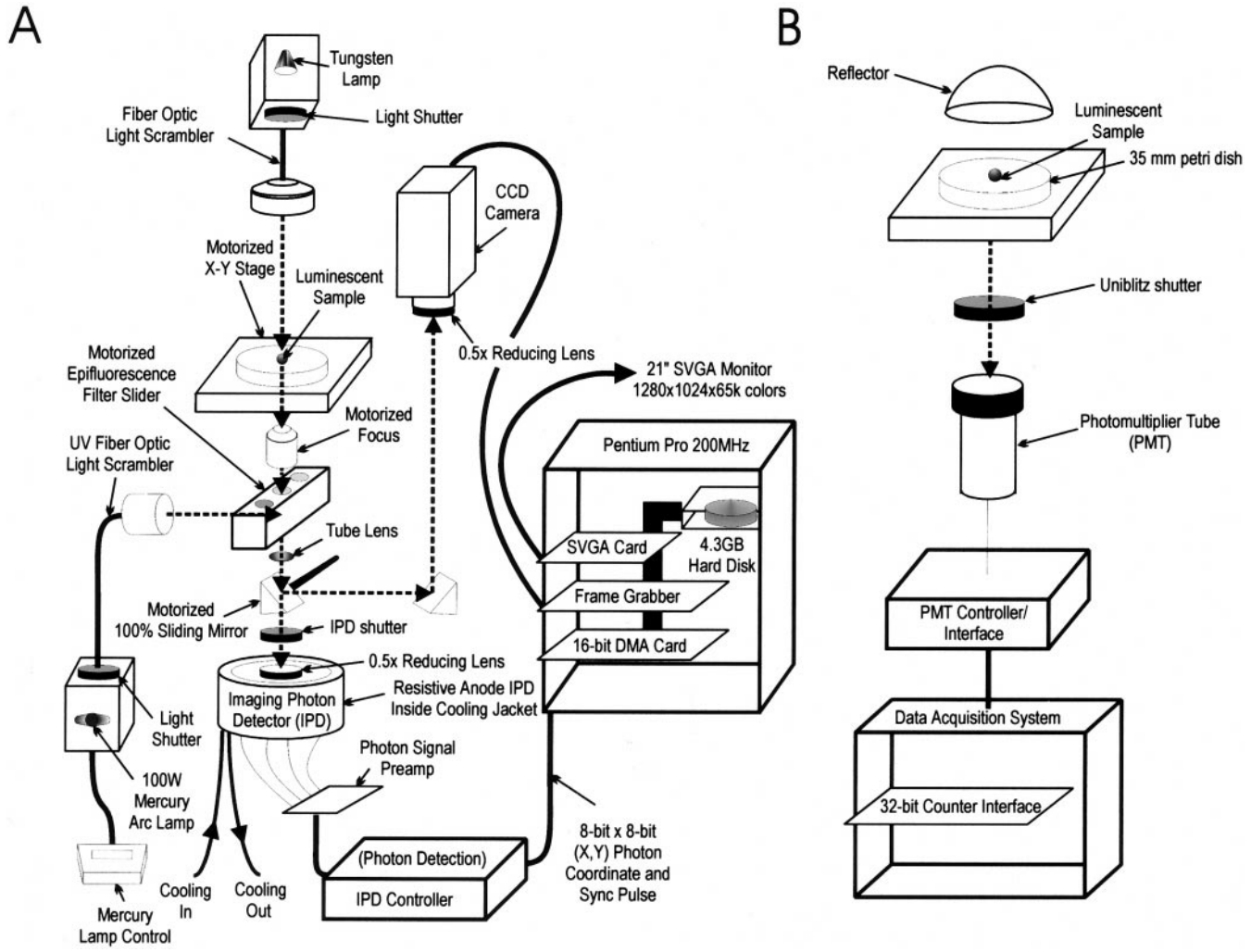

FIG. 2. Schematic outline of our (A) photon imaging microscope system for details see Webb *et al.* (1997) and (B) photo-multiplier tube-based photon counting system.

camera (TK-C1381; JVC) mounted on a stereomicroscope (Stemi SV6; Zeiss), with images recorded on a VCR (AG-6750; Panasonic). Images were then exported to Metamorph 3.0 for data analysis. Three aspects of the activation process were analyzed both in the presence and in the absence of sperm: the timing of activation events (i.e., the onset of the cortical granule reaction, followed by chorion elevation); the nature of the cortical granule reaction during the activation process; and an estimation of size changes of eggs following activation.

RESULTS

Calcium Wave Velocities

Figure 3 shows a representative example ($n = 4$) of a calcium wave traversing a zebrafish egg following activation in the absence of sperm. For imaging purposes, this particular egg was in a perfect side-on orientation, with the animal pole (AP) located at the left-hand side. This made analyzing the velocity of the wave easy using the "Line-scan" function in Metamorph 3.0. A plot of wavefronts at three separate times is illustrated in Fig. 5A, indicating a cortical velocity along the AP to vegetal pole (VP) axis of approximately 9 μm/s. When comparing bright-field images before and after activation (i.e., Figs. 3A and 3K, respectively), the chorion was clearly elevated by the time the calcium wave had traversed the egg. Eggs activated in this manner segregated normally to form a blastodisc and then attempted abortive cleavages. They did not, however, develop any further.

Figure 4 illustrates a representative example ($n = 3$) of a calcium wave in an egg activated in the presence of sperm, which was then subsequently seen to have been

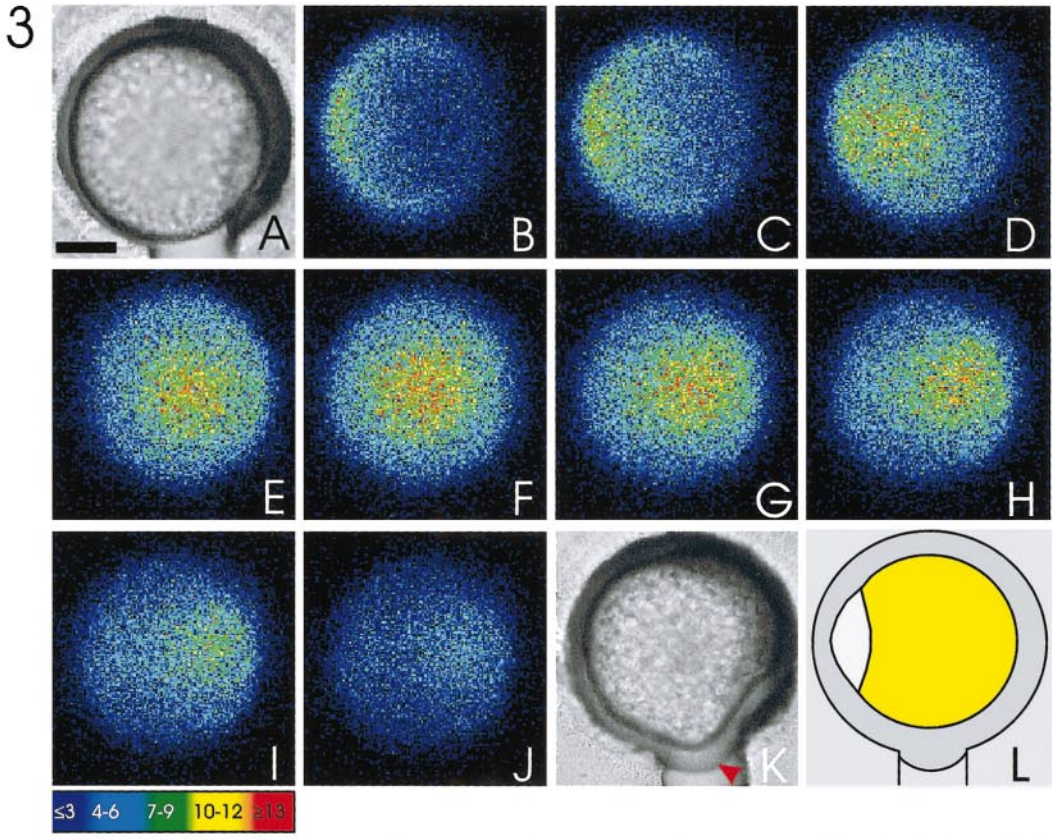

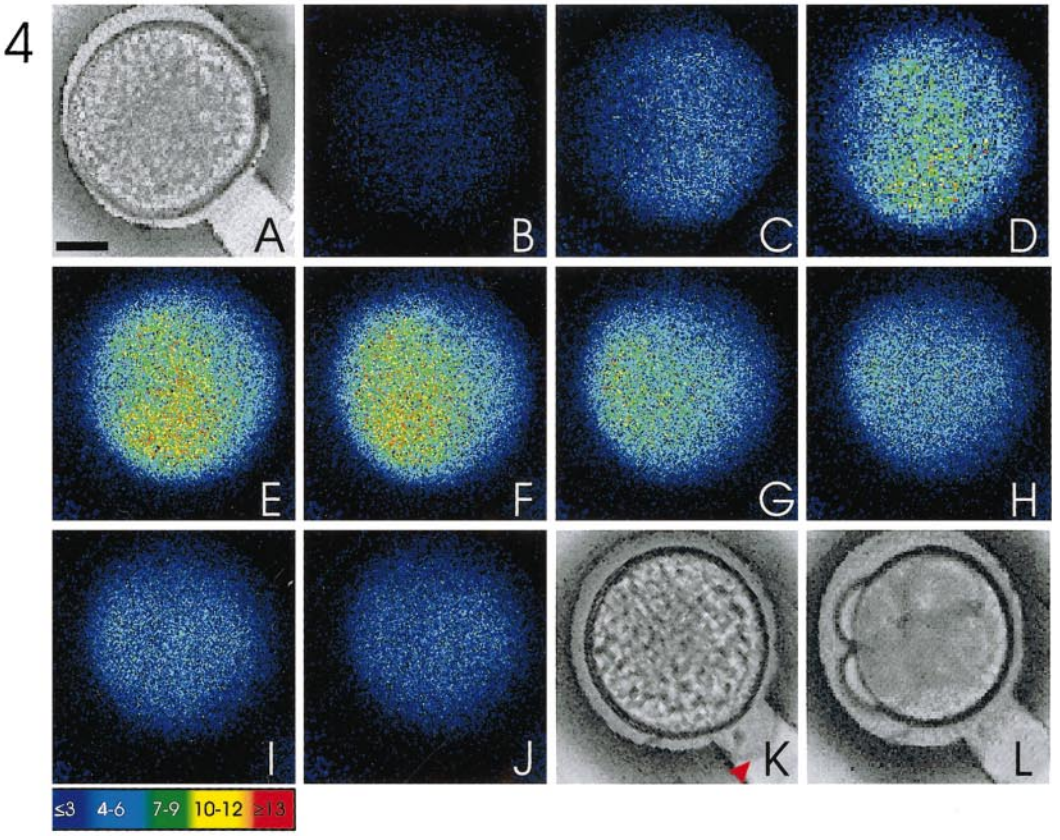

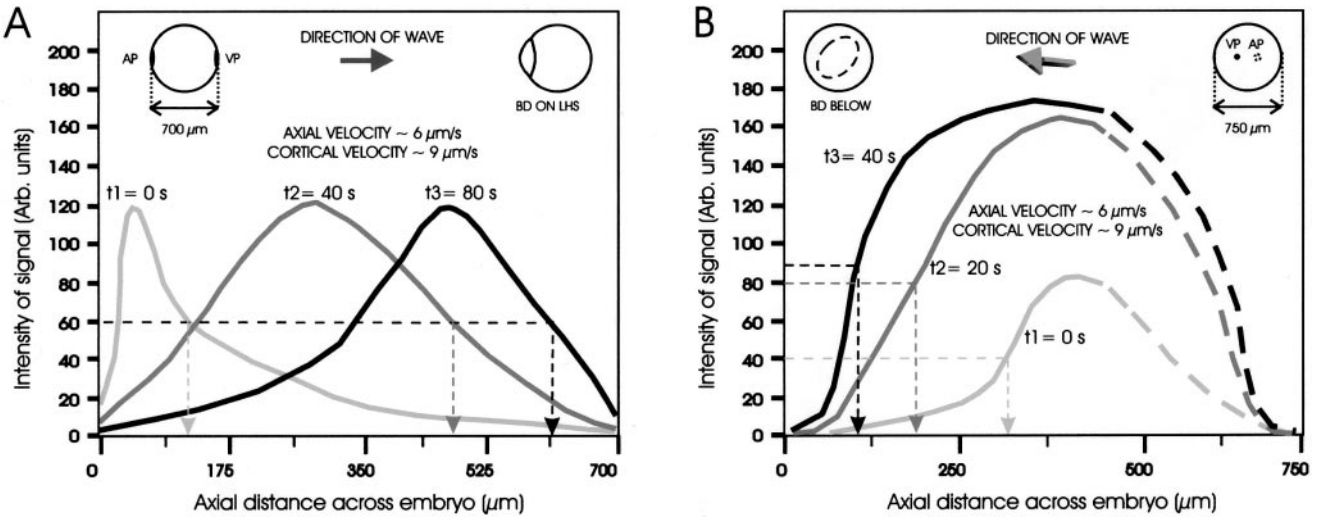

FIG. 5. Analysis of the sequences of images shown in Figs. 3 and 4. Profiles of the intensity of photon emission were measured using the Linescan function of Metamorph 3.0. Line lengths of 700 and 750 μm were used, as these were the diameters of the eggs in Figs. 3 and 4, respectively. Each profile shows the relative intensity of photons collected for 60 s. Profiles for activation in the absence of sperm (A) were taken from Figs. 3D, 3F, and 3H. Profiles generated in the presence of sperm (B) were taken from Figs. 4C, 4D, and 4E. Schematic diagrams in the top corners of A and B show subsequent blastodisc (BD) formation and thus the location of the AP during wave propagation. The broken profile lines in B indicate that only the left-hand side of this plot was used to calculate a wave velocity (see Results). The dashed lines indicate the half-heights used as an arbitrary indication of the position of the wave fronts at each time point. The Linescan analysis assumes that the wave passes directly through the egg along the AP to VP axis; thus we refer to this value as the axial velocity. These are converted to a cortical velocity, which assumes that the wave travels the hemicircumference distance between the AP and the VP (i.e., this equals approximately 1100 and 1178 μm for the 700- and 750-μm-diameter eggs in A and B, respectively). AP and VP are the animal and vegetal poles, respectively.

fertilized as it went on to divide and develop normally (see Fig. 4L). In this example, the egg is not in a perfect side-on orientation for imaging, as its AP is tilted slightly to the right and beyond the focal plane of the image (see the schematic in Fig. 5B). There is no clear morphological indicator of the AP or VP in unfertilized zebrafish eggs. Thus, the most reliable polarity marker is the eventual location of the forming blastodisc, assuming that the egg does not move or rotate during activation and early segregation. Unfertilized eggs were therefore loaded into the injection chambers in a random orientation and as a result, we never imaged an egg activated and fertilized in the presence of sperm in a perfect side-on orientation such as the egg illustrated in Fig. 3. The orientation of the egg shown in Fig. 4 led us therefore to use only the left-hand side of the egg to generate the wave-front plots indicated in Fig. 5B (the right-hand side of the plots are represented by broken lines). This analysis once again reveals a cortical wave velocity of around 9 μm/s. In both Figs. 5A and 5B we used the half-height of the advancing

FIG. 3. Representative sequence of images from an aequorin-loaded egg illustrating changes in intracellular free calcium during activation in the *absence* of sperm. A is a bright-field image of the unactivated egg just prior to the initiation of the signal and shows no separation between the chorion and the egg plasma membrane, whereas K shows the egg after the passage of the calcium wave, clearly indicating (arrowhead) a raised chorion. Each photon image (B to J) represents 60 s of accumulated light, with a 20-s step separating each successive image. The schematic image (L) shows subsequent blastodisc (in white) formation and thus the location of the animal pole during wave propagation. The egg developed only as far as a few abortive cleavages. Color scale indicates luminescent flux in photons per pixel. Scale bar is 200 μm.

FIG. 4. Representative sequence of images from an aequorin-loaded egg illustrating changes in intracellular free calcium during activation in the *presence* of sperm. A is a bright-field image of the unactivated egg just prior to the initiation of the signal and once again shows no separation between the chorion and the egg plasma membrane, whereas K shows the egg after the passage of the calcium wave, clearly indicating (see arrowhead) a raised chorion. L shows the egg at the 4-cell stage, indicating that it has been fertilized and is developing normally. The photon images (B to J) represent 60 s of accumulated light, with a 20-s step separating each successive image. The dividing blastodisc in L indicates the location of the AP. Color scale indicates luminescent flux in photons per pixel. Scale bar is 200 μm.

TABLE 1
Data Summary from the PIM and PMT Experiments

	Activation without sperm	Activation with sperm
From PIM experiments		
Cortical Ca^{2+} wave velocity	8.9 ± 0.8 μm/s (n = 4)	9.0 ± 0.2 μm/s (n = 3)
Wave initiation site	Animal pole	Animal pole
Cortical granule reaction	Yes	Yes
Chorion elevation	Yes	Yes
Ooplasmic segregation	Yes	Yes
Cleavage	No	Yes
Normal development	No	Yes
From PMT experiments		
Duration of luminescence pulse	7.1 ± 2.0 min (n = 12)	7.4 ± 1.2 min (n = 3)
Rise time to luminescence peak	1.0 ± 0.5 min (n = 12)	0.7 ± 0.1 min (n = 3)
Ratio of Ca^{2+} rise above resting level (√ luminescence)	138.0 ± 21.8-fold (n = 3)	116.4 ± 11.0-fold (n = 3)

Note. Values represent mean ± standard deviation.

wave front in our calculation. Mean wave velocities for all experiments are given in Table 1.

Where it was possible (for example, in eggs orientated as shown in Fig. 3), we also compared the wave propagation velocity in the animal and vegetal hemispheres under both experimental conditions. The velocity of propagation was consistently found to be higher in the animal hemisphere compared to the vegetal—for example, in the case of the egg shown in Fig. 3 they were calculated to be 10.2 and 6.3 μm/s, respectively. Whether activated in the presence or in the absence of sperm, all waves were initiated from around the AP, the site of the micropyle.

Durations, Rise Times, Profiles, and Peaks of Calcium Transients

A comparison of the characteristics of activation in the presence and in the absence of sperm is summarized in Table 1. Figure 6 compares the profile, duration, and extent of the aequorin-generated luminescence in two representative examples of eggs activated in the absence (Figs. 6A and 6C) or in the presence of sperm (Figs. 6B and 6D). We consider differences in peak height not to be meaningful as they result from experimental variation. These data were collected using our PMT system (see Fig. 2B) and are included in the data summary presented in Table 1 (eggs activated in the absence of sperm, n = 12; in the presence of sperm, n = 3). Like the wave propagation velocities described in the previous section, the profiles of the egg responses under the two activation conditions appear very similar. The higher time resolution plots of the initiation of the transients shown in Figs. 6C and 6D indicate that under both conditions there is an initial period (of a few seconds) where there is a slow increase in luminescent output. This is followed by the main explosive rise, which again is very similar under the two experimental conditions. To estimate the ratio of the calcium rise above the resting level we compared the level of luminescence at the peak of the activation response with the resting level before activation (Table 1). Figure 6C′ is modified from Fig. 3B to show just the first 10 s of luminescence during the activation response and illustrates that the initial slow luminescent increase is localized to a region surrounding the micropyle in the animal hemisphere cortex.

Wave Propagation Pathway

The VP view of a representative activation wave illustrated in Fig. 7 (n = 4) indicates that the wave appears to propagate mainly through the periphery of the egg in the yolk-free cortex. It also suggests that the level of free Ca^{2+} in the deep interior of the egg also seems to rise during the propagation of the wave, but not to the same extent as in the cortex.

Rotational Movements during Activation

Our data indicate that zebrafish eggs do not rotate once the chorion has separated from the plasma membrane during the activation process. Figure 8 (a representative example, n = 3) clearly indicates that fluorescent Nile red microspheres injected into the periphery of an unactivated egg maintain their general position throughout the activation process (i.e., for at least 5 min).

Activation in Calcium-Free Medium

When eggs were collected in calcium-free 0.5% BSA in Hank's saline, they activated within 5 min (n = 30; data not shown). These experiments indicated two factors: that external calcium was required to maintain the eggs in an unactivated condition and that the calcium both initiating

and generating the activation signal can be provided entirely from internal stores.

Video Analysis of Egg Activation

A close analysis of real-time video recordings using Metamorph 3.0 indicated that when comparing activation either in the absence or in the presence of sperm, there were no significant qualitative or quantitative differences in the activation events. In both cases the onset of the CG reaction followed by chorion elevation occurred approximately 30 s after the addition of the activating medium. We also confirmed the observation of Hart and Yu (1980) that the CG reaction in zebrafish eggs occurs all over the surface of the egg at approximately the same time; i.e., there is not a distinct wave of CG fusion and exocytosis as displayed by medaka eggs (Gilkey *et al.*, 1978). This near-simultaneous exocytosis was observed under both activation regimes (data not shown). Finally, changes in the diameter of eggs initiated by the activation process were the same (i.e., an approximate reduction in diameter of 15%) under both activation conditions.

DISCUSSION

Activation Followed by Fertilization

We observed no striking differences between the calcium waves generated by eggs activated by the spawning medium in the absence of sperm and those subsequently shown (in the presence of sperm) to be fertilized. This leads us to suggest that sperm do not compete with the spawning medium to activate zebrafish eggs, rather that normally the eggs are first activated by the spawning medium and then fertilized. Here we define activation to be the initiation of an explosive rise in intracellular calcium that propagates across the egg in a wave-like manner and which results in the resumption of the dormant egg's metabolism. Fertilization is defined as the union of gametes followed by the subsequent steps that lead to the restoration of the diploid genome.

In the natural situation where a male and female fish simultaneously discharge eggs and milt into the spawning medium, their breeding behavior brings the gametes together in a matter of seconds. Indeed, *in vitro* studies have reported zebrafish sperm to be attached to the microvilli of the sperm entry site at the egg micropyle within 5 to 10 s after insemination (Wolenski and Hart, 1987). Thus, although we are making a distinction between activation and fertilization, it is clear that these two events are normally separated by perhaps only a few to tens of seconds. Once the CG reaction is initiated and the chorion begins to rise, some 30 s after the first morphological signs of activation in zebrafish (Hart and Yu, 1980), sperm are no longer able to reach the plasma membrane through the micropyle and a short but lethal program of parthenogenetic development is initiated. In summary, we suggest that eggs are initially activated by the spawning medium and there then follows a restricted window of opportunity (probably less than 30 s—but perhaps only between 5 and 10 s) for sperm to fertilize the egg. This strategy helps to ensure that only sperm from the successful male paired with the spawning female fertilizes her eggs. Presumably the behavioral-mediated selection of breeding partners followed by this fertilization strategy confers some selective advantage to the zebrafish progeny.

This is, however, an activation/fertilization strategy somewhat different than that described for medaka (Gilkey *et al.*, 1978; Yoshimoto *et al.*, 1986; Iwamatsu *et al.*, 1988). Thus, as first suggested some 40 years ago by Rothschild (1958), this study of a different teleost species is revealing interesting variations that may help to further our understanding of fertilization in vertebrates.

Zebrafish do not represent an isolated case as a similar strategy has been reported with regard to the activation of eggs of other fish species such as goldfish (*Carassius auratus*) and the pond smelt (*Hypomesus olidus;* Yamamoto, 1954). Furthermore, the marine shrimp *Sicyonia ingentis* (Lindsay *et al.*, 1992) and the prawn *Palaemon serratus* (Goudeau and Goudeau, 1996) also display this strategy, and in both cases it has been reported that the initiation of a calcium activation wave once again does not require sperm. Instead, these eggs are activated when they are exposed to seawater Mg^{2+} during spawning. In both cases, if eggs remain unfertilized, they will still resume meiosis, form a hatching envelope, and eventually (in the case of *S. ingentis*) undergo abnormal cleavage (Pillai and Clark, 1987; Goudeau *et al.*, 1991). This maternally derived developmental program is very similar to that observed in zebrafish. It has also been determined that for both crustacean species external Ca^{2+} is not required for the Mg^{2+}-induced activation wave. Once again, this is similar to zebrafish for which we report that external calcium is likewise not required to generate an activation wave. The presence of external calcium is, however, required (in 0.5% BSA in Hank's buffered saline) to maintain eggs in an unactivated state for any period of time.

Wave Initiation Point

In situations in which sperm are thought to normally activate mature fish eggs, such as in the case of the medaka, it is from the point of sperm contact (i.e., at the micropyle) that the calcium wave (Gilkey *et al.*, 1978), the wave of CG extrusion (Yoshimoto *et al.*, 1986), and chorion elevation (Yamamoto, 1961) begin. In the case of activation in the absence of sperm in zebrafish, we report that the calcium wave appears to be still initiated from the micropyle region at the AP. This might be due to the fact that spawning medium (and/or any activating factor in it) makes contact with the egg plasma membrane more rapidly via the micropyle than through the chorion (Hart, 1990). Furthermore, it has been reported that in zebrafish there is a "tuft" of plasma membrane-derived microvilli at the micropyle to

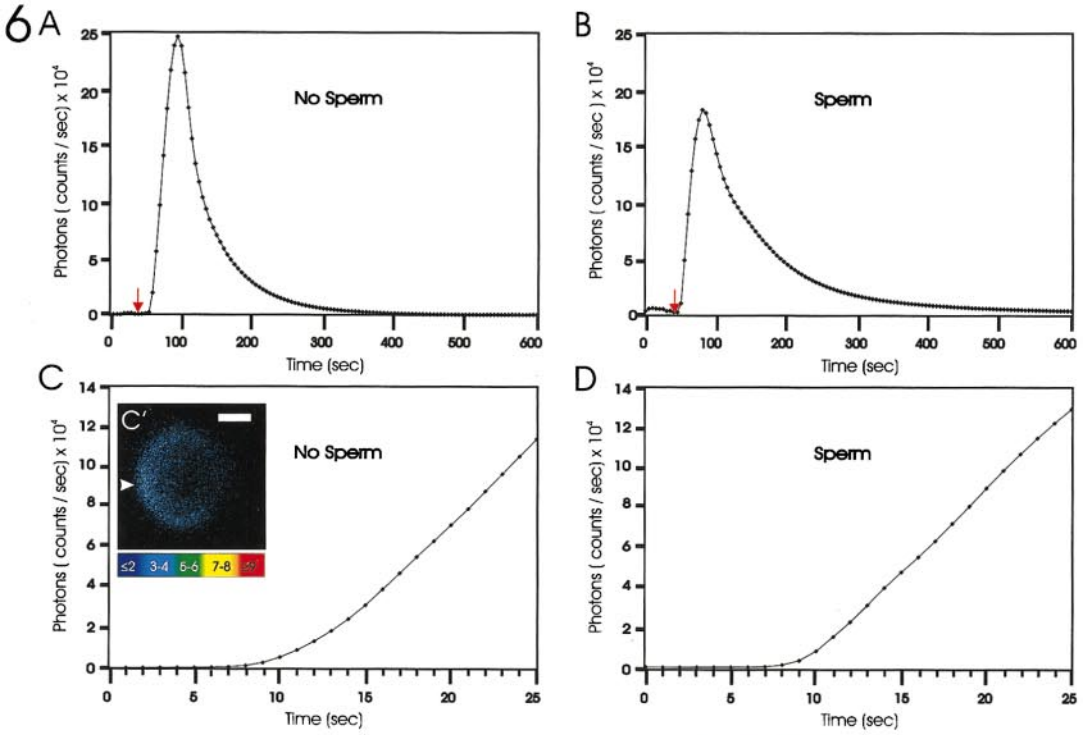

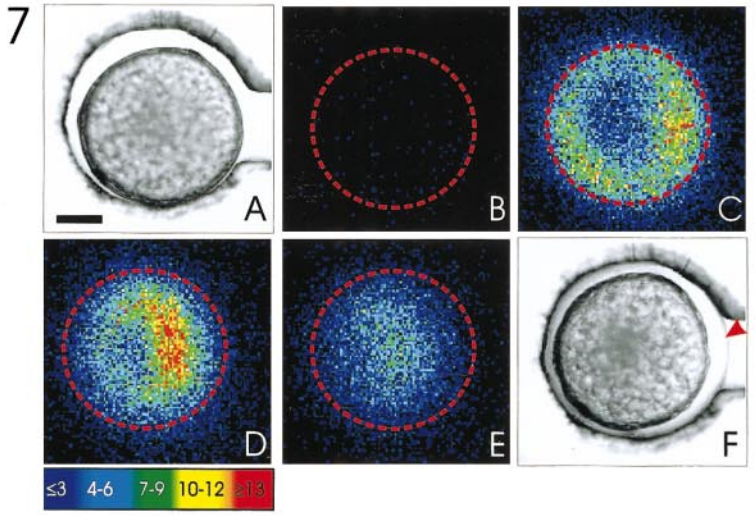

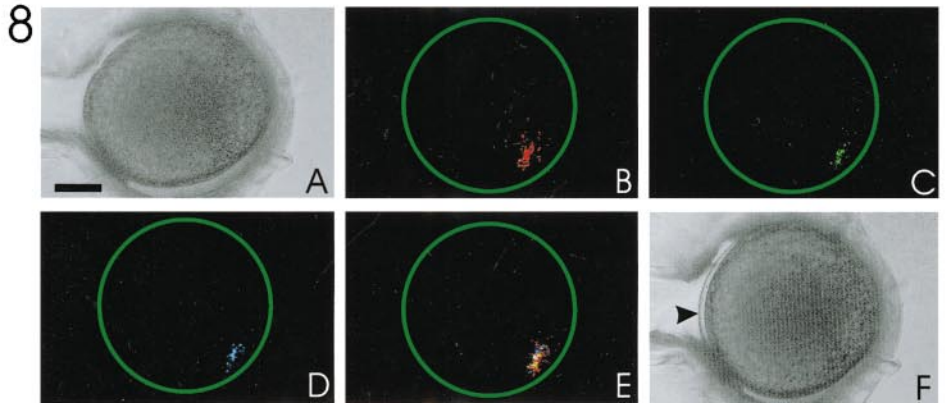

which a sperm head eventually binds (Hart and Yu, 1980). This tuft might also serve to increase the surface area of the plasma membrane coming in contact with the spawning medium, resulting in an amplification of a triggering signal, thus ensuring that the calcium wave is initiated from this location. Another morphological feature that may favor initiation of the calcium wave at the micropyle is the presence of an extensive array of ER beneath the plasma membrane at this location (Hart, 1990). It has been suggested that the ER is the calcium store required both to initiate and to propagate calcium activation waves (Jaffe, 1991).

Path of Wave Propagation through the Egg

In the medaka the calcium wave is propagated only through the peripheral cytoplasm of the egg (Gilkey *et al.*, 1978). In this species, the interior of the egg is filled with a single, large membrane-bound yolk compartment. In the zebrafish, the morphology of yolk encapsulation is somewhat different due to the presence of many membrane-bound yolk globules (Beams *et al.*, 1985). These, however, are excluded from the outermost 15 to 20 μm of the egg, resulting in a functional yolk-free cortex (Hart, 1990). Our aequorin-generated data suggest that in zebrafish the activation wave also propagates mainly through the cortex (see Fig. 7) rather than through the whole egg. This suggestion is supported by observations regarding egg morphology. In addition to the array beneath the micropyle, the ER in the zebrafish cortex forms an extended peripheral network and has been reported to form intimate contacts between both the plasma membrane and the membranes of the CGs (Beams and Kessel, 1973). Thus, the egg cortex possesses the structural element (i.e., an ER Ca^{2+} store) suggested necessary to propagate a CICR wave (Jaffe, 1991). On the other hand, it is not clear whether such a wave-propagating network of ER extends through the deep interior of the zebrafish egg, thus connecting the restricted and convoluted interglobule space in the same way as it does in the cortex. One also must consider other elements of the wave propagation mechanism, such as the distribution of the required calcium-release channels, when comparing peripheral domains of ER to deep domains (Gillot and Whitaker, 1993).

Activation Wave Velocity

Our method of analyzing activation wave velocities using the Linescan function of Metamorph (see Materials and Methods) result in "axial velocities"; i.e., it assumes that the wave passes directly through the egg along the AP to the VP axis. As discussed in the previous section, our imaging data suggest that the propagating calcium wave passes mainly through the cortex of the egg, i.e., a distance more like the hemicircumference rather than the diameter of the egg. Thus, we corrected our Linescan-derived axial velocity values to reflect this, calling them "cortical velocities" (see Fig. 6 and Table 1). This correction results in wave velocities of around 9 μm/s for eggs activated either in the presence or in the absence of sperm, which is in the same range as the ionomycin-induced activation waves reported previously in zebrafish (Lee *et al.*, 1996). These velocities clearly fall into the category of "fast" calcium activation waves proposed by Jaffe (1993). Thus, zebrafish are another species that displays a highly conserved calcium activation wave velocity, perhaps suggesting a common mechanism of wave propagation in both deuterostomes (Jaffe, 1991; Jaffe and Créton, 1998) and protostomes (Eckberg and Miller, 1995; Stricker, 1996).

Estimation of Peak Calcium Levels during Wave Propagation

The aequorin-generated data from our PMT system indicate that there is an approximate 10,000-fold difference in

FIG. 6. Representative profiles of luminescence from aequorin-loaded eggs activated either in the absence (A and C) or in the presence (B and D) of sperm. These data were gathered using our PMT system. A and B illustrate plots (every 5 s) of the total luminescent output for the entire activation process. C and D show luminescent output at a higher temporal resolution (every 1 s), indicating an initial period (around 3–5 s) of lower level emission prior to the explosive rise. Red arrows in A and B indicate the addition to the egg-injection chamber of either 0.5% fructose in egg-water (A) or 0.5% fructose in egg-water 30 s after the addition of concentrated sperm suspension (B). C′ illustrates the first 10 s of the activation response of the egg shown in Fig. 3, indicating the initial low-intensity localized response around the micropyle (arrowhead) in the animal hemisphere. Color scale indicates luminescent flux in photons per pixel. Scale bar is 200 μm.

FIG. 7. Representative series of images of a vegetal pole (VP) view of an activation wave indicating that the wave propagates mainly in the periphery of the egg. A and F are bright-field images of the egg before and after activation, respectively. The arrowhead in F indicates the raised chorion. B illustrates the resting level of luminescence prior to activation. C indicates the activation wave at the equator of the egg, and D and E demonstrate the subsequent progression of the wave to the VP. The location of the egg equator is outlined. B to E show 60 s of accumulated light. Color scale indicates luminescent flux in photons per pixel. Scale bar is 200 μm.

FIG. 8. A representative example of a zebrafish egg with fluorescent microspheres loaded into its periphery. A and F are bright-field images taken before and after activation, respectively. A shows no separation between the chorion and the egg plasma membrane, whereas in F, the chorion is clearly raised (see arrowhead). B to D indicate confocal images taken at an optical plane containing the fluorescent microspheres. The fluorescent image in B was taken before the addition of 0.5% fructose in egg-water and then C and D at 2.5 and 5 min later, respectively. E shows the fluorescent images from B, C, and D superimposed on one another. This demonstrates that the egg does not rotate within its expanding chorion during the activation process. Scale bar is 200 μm.

luminescence at the peak of the activation response, compared to the resting level before activation (see Fig. 6 and Table 1). If we assume that the luminescence of *f*- and *h*-aequorin varies with the calcium concentration *in vivo* as it does *in vitro*, i.e., to the second power (Shimomura, 1995), this represents a 100-fold difference in the levels of cytosolic free calcium. If we use a value of around 60 nM reported by Créton *et al.* (1998) for the resting level of cytosolic free calcium in fertilized zebrafish eggs, then we obtain a peak calcium rise of around 6 μM. Thus, our estimation of the peak calcium rise during the activation wave in zebrafish is 5-fold less than that estimated for medaka, i.e., around 30 μM (Gilkey *et al.*, 1978), but very much in line with levels reported for a variety of sea urchin species (see Table III in Browne *et al.*, 1996).

Activation Does Not Block Fertilization

One essential element in our proposal that zebrafish eggs are activated by their spawning medium and then subsequently fertilized is that the prefertilization activation response does not induce an electrically mediated block to sperm–egg fusion. Is there any evidence for this? From voltage-clamping experiments, Nuccitelli (1980) showed that the membrane potential of the medaka egg shifts only slightly on fertilization for a period of about 20 s. Furthermore, he reported that voltage clamping an egg's membrane potential between −80 and +48 mV did not prevent fertilization. This observation is contrary to the fast electrically mediated block to polyspermy that has been reported in a number of invertebrate and vertebrate eggs (Miyazaki and Hirai, 1979; Jaffe and Gould, 1985). Thus, fertilization in medaka eggs is not inhibited by a rapid, positive membrane potential at the plasma membrane. If a similar situation exists in zebrafish, this would help to support our proposal that after eggs have been activated by the spawning medium, they can still be fertilized by a sperm when sperm are present. Monospermy in zebrafish is guaranteed by a morphological strategy (rather than an electrical strategy) in which the spherical head of the fertilizing sperm is around 2.5–2.8 μm in diameter, while the inner aperture of the micropylar canal is only slightly larger (Hart and Donovan, 1983). Thus, since two spermatozoa cannot pass simultaneously through the inner micropylar aperture, the block to polyspermy in zebrafish would appear to be relatively fast, mechanical, and mediated by the first sperm to reach the egg surface (Hart, 1990).

Relationship between Calcium Wave and CG Breakdown

There appear to be at least two distinctive patterns of CG breakdown in teleost eggs. For example, in medaka (Gilkey *et al.*, 1978) and *Fundulus* (Brummett and Dumont, 1981), the exocytosis of CGs begins at the AP, at or close to the micropyle. It then propagates in a wave-like fashion over the egg surface to the antipode at the VP. In the case of medaka, the wave of cortical CG fusion follows approximately 17 s after the propagating calcium wave (Yoshimoto *et al.*, 1986). However, a second pattern occurs in eggs of zebrafish where CG exocytosis is not initiated at the AP and does not propagate from there in a wave-like fashion. In this case, after a delay of about 30 s following activation, the CG reaction is initiated randomly and more or less simultaneously over the egg surface (Hart and Yu, 1980; Schalkoff and Hart, 1986).

The organization, arrangement, and size of CGs, however, also appear to be variable in the eggs of teleosts. In medaka they are approximately 10–40 μm in diameter and form a tightly packed monolayer in the cortical cytoplasm (Gilkey *et al.*, 1978). By contrast, the CGs of zebrafish tend to be smaller (between 3 and 22 μm in diameter) and are arranged in several irregular layers throughout most of the cortex. Furthermore, the granules in these layers are organized in a gradient of progressively increasing size from the AP to the VP (Hart and Donovan, 1983). We suggest, therefore, that the different relationship between the calcium activation waves and the process of CG to plasma membrane fusion in these two species may be related to these morphological differences in their CG arrangements. The duration of the cytosolic calcium elevation resulting from the activation wave in zebrafish (some 7 min, see Table 1) does, however, correlate well with the time required to complete the CG reaction and elevate the chorion (i.e., around 6 min; Hart and Yu, 1980).

Possible Mechanism for Triggering the Activation Wave

At the moment, we do not know the exact mechanism through which the spawning medium triggers the activating calcium wave. However, it clearly does not involve any sperm-derived factors as suggested for other systems (Swann, 1993). Thus, the situation in zebrafish is quite unlike that found for example in the mouse, where sperm–egg fusion must occur before the calcium transient is initiated and where intracellular transients are never observed under any conditions in the absence of sperm–egg fusion (Lawrence *et al.*, 1997). In mouse, however, activation involves multiple calcium oscillations (Swann, 1994), whereas in zebrafish it requires only a single propagating transient. Perhaps some sperm-derived factor is required for maintaining multiple oscillations (Parrington *et al.*, 1996; Swann and Lai, 1997).

Our data suggest (see Figs. 6C, 6C′, and 6D) that there is a slow localized build-up of intracellular calcium for a few seconds prior to the explosive propagating calcium wave. We have already mentioned the extensive ER network located at the micropyle (Hart, 1990), which we would suggest is the store responsible for this initial calcium release that eventually triggers the wave. The fact that eggs can be activated when bathed in calcium-free medium would appear to eliminate calcium itself as the diffusible messenger entering the egg via the micropyle and stimulat-

ing the intracellular calcium release (Créton and Jaffe, 1995). This leaves the possibility of some transmembrane receptor generating a calcium release agent as a reasonable suggestion for a triggering mechanism. In the case of the Mg^{2+}-activated shrimp egg, Lindsay *et al.* (1992) suggest that a Mg^{2+}-sensitive receptor linked to a G-protein-based signal transduction pathway generates inositol 1,4,5-trisphosphate (IP_3), which in turn stimulates the initiation and propagation of the calcium wave. There is some evidence supporting this idea, in that another external divalent cation (i.e., cadmium) has been shown to increase intracellular IP_3 and Ca^{2+} levels (Smith *et al.*, 1989).

ACKNOWLEDGMENTS

We thank Dr. Nathan Hart for his critical comments and helpful suggestions. We also thank Drs. O. Shimomura, Y. Kishi, and S. Inouye for generously supplying us with *f*- and *h*-aequorin. This work was supported by Hong Kong RGC Grant HKUST 650/96M awarded to A.L.M. and DAG97/98.SC09 awarded to A.L.M. and S.E.W., and equipment was donated by the Hong Kong Jockey Club.

REFERENCES

Albrieux, M., Sardet, C., and Villaz, M. (1997). The two intracellular Ca^{2+} release channels, ryanodine receptor and inositol 1,4,5-trisphosphate receptor, play different roles during fertilization in ascidians. *Dev. Biol.* **189,** 174–185.

Beams, H. W., and Kessel, R. G. (1973). Oocyte structure and early vitellogenesis in the trout, *Salmo gairdneri. Am. J. Anat.* **136,** 105–121.

Beams, H. W., Kessel, R. G., Shih, C. Y., and Tung, H. N. (1985). Scanning electron microscope studies on blastodisc formation in the zebrafish, *Brachydanio rerio. J. Morphol.* **184,** 41–49.

Browne, C. L., Créton, R., Karplus, E., Mohler, P. J., Palazzo, R. E., and Miller A. L. (1996). Analysis of the calcium transient at NEB during the first cell cycle in dividing sea urchin eggs. *Biol. Bull.* **191,** 5–16.

Brummett, A. R., and Dumont, J. N. (1981). Cortical vesicle breakdown in fertilized eggs of *Fundulus heteroclitus. J. Exp. Zool.* **216,** 63–79.

Busa, W. B., and Nuccitelli, R. (1985). An elevated free cytosolic Ca^{2+} wave follows fertilization in eggs of the frog, *Xenopus laevis. J. Cell Biol.* **100,** 1325–1329.

Corley-Smith, G. E., Lim, C. J., and Brandhorst, B. P. (1996). Production of androgenetic zebrafish (*Danio rerio*). *Genetics* **142,** 1265–1276.

Créton, R., and Jaffe, L. F. (1995). Role of calcium influx during the latent period in sea urchin fertilization. *Dev. Growth Differ.* **37,** 703–709.

Créton, R., Speksnijder, J. E., and Jaffe, L. F. (1998). Patterns of free calcium in zebrafish embryos. *J. Cell Sci.* **111,** 1613–1622.

Digonnet, C., Aldon, D., Leduc, N., Dumas, C., and Rougier, M. (1997). First evidence of a calcium transient in flowering plants at fertilization. *Development* **124,** 2867–2874.

Eckberg, R. E., and Miller, A. L. (1995). Propagated and nonpropagated calcium transients during egg activation in the annelid, *Chaetopterus. Dev. Biol.* **172,** 654–664.

Epel, D. (1990). The initiation of development at fertilization. *Cell Differ. Dev.* **29,** 1–12.

Galione, A., McDougall, A., Busa, W. B., Willmott, N., Gillot, I., and Whitaker, M. (1993). Redundant mechanisms of calcium-induced calcium release underlying calcium waves during fertilization of sea urchin eggs. *Science* **261,** 348–352.

Gilkey, J. C., Jaffe, L. F., Ridgway, E. B., and Reynolds, G. T. (1978). A free calcium wave traverses the activating egg of the medaka, *Oryzias latipes. J. Cell Biol.* **76,** 448–466.

Gillot, I., and Whitaker, M. (1993). Imaging calcium waves in eggs and embryos. *J. Exp. Biol.* **184,** 213–219.

Goudeau, M., and Goudeau, H. (1996). External Mg^{2+} triggers oscillations and a subsequent sustained level of intracellular free Ca^{2+}, correlated with changes in membrane conductance in the oocyte of the prawn *Palaemon serratus. Dev. Biol.* **177,** 178–189.

Goudeau, M., Goudeau, H., and Guillaumin, D. (1991). Extracellular Mg^{2+} induces a loss of microvilli, membrane retrieval, and the subsequent cortical reaction, in the oocyte of the prawn *Palaemon serratus. Dev. Biol.* **148,** 31–50.

Hart, N. H. (1990). Fertilization in teleost fishes: Mechanisms of sperm–egg interactions. *Int. Rev. Cyt.* **121,** 1–66.

Hart, N. H., and Donovan, M. (1983). Fine structure of the chorion and site of sperm entry in the egg of *Brachydanio. J. Exp. Zool.* **227,** 277–296.

Hart, N. H., and Fluck, R. A. (1995). Cytoskeleton in teleost eggs and early embryos: Contributions to cytoarchitecture and motile events. *Curr. Top. Dev. Biol.* **31,** 343–381.

Hart, N. H., and Yu, S. F. (1980). Cortical granule exocytosis and cell surface reorganization in eggs of *Brachydanio. J. Exp. Zool.* **213,** 137–159.

Hisaoka, K. K., and Firlit, C. F. (1962). Ovarian cycle and egg production in the zebrafish, *Brachydanio rerio. Copeia* **4,** 788–792.

Homa, S. T., and Swann, K. (1994). A cytosolic sperm factor triggers calcium oscillations and membrane hyperpolarizations in human oocytes. *Hum. Reprod.* **9,** 2356–2361.

Iwamatsu, T., Yoshimoto, Y., and Hiramoto, Y. (1988). Cytoplasmic Ca^{2+} release induced by microinjection of Ca^{2+} and effects of microinjected divalent cations on Ca^{2+} sequestration and exocytosis of cortical alveoli in the medaka egg. *Dev. Biol.* **125,** 451–457.

Jaffe, L. A., and Gould, M. (1985). Polyspermy-preventing mechanisms. *In* "Biology of Fertilization" (C. B. Metz and A. Monroy, Eds.), Vol. 3, pp. 223–250. Academic Press, Orlando, FL.

Jaffe, L. F. (1985). The role of calcium explosions, waves, and pulses in activating eggs. *In* "Biology of Fertilization" (C. B. Metz and A. Monroy, Eds.), Vol. 3, pp. 127–165. Academic Press, Orlando, FL.

Jaffe, L. F. (1991). The path of calcium in cytosolic calcium oscillations: A unifying hypothesis. *Proc. Natl. Acad. Sci. USA* **88,** 9883–9887.

Jaffe, L. F. (1993). Classes and mechanisms of calcium waves. *Cell Calcium* **14,** 736–745.

Jaffe, L. F., and Créton, R. (1998). On the conservation of calcium wave speeds. *Cell Calcium* **24,** 1–8.

Kimmel, C. B., Ballard, W. W., Kimmel, S. R., Ulmann, B., and Schilling, T. F. (1995). Stages of embryonic development of the zebrafish. *Dev. Dyn.* **203,** 253–310.

Kline, D., and Kline, J. T. (1992). Repetitive calcium transients and the role of calcium in exocytosis and cell cycle activation in the mouse egg. *Dev. Biol.* **149,** 80–89.

Kubota, H. Y., Yoshimoto, Y., Yoneda, M., and Hiramoto, Y. (1987). Free calcium wave upon activation in *Xenopus* eggs. *Dev. Biol.* **119,** 129–136.

Lawrence, Y., Whitaker, M., and Swann, K. (1997). Sperm–egg fusion is the prelude to the initial Ca^{2+} increase at fertilization in the mouse. *Development* **124,** 233–241.

Lee, K. W., Baker, R., Galione, A., Gilland, E. H., Hanlon, R. T., and Miller, A. L. (1996). Ionophore-induced calcium waves activate unfertilized zebrafish (*Danio rerio*) eggs. *Biol. Bull.* **191,** 265–267.

Lindsay, L. L., Hertzler, P. L., and Clark, W. H., Jr. (1992). Extracellular Mg^{2+} induces an intracellular Ca^{2+} wave during oocyte activation in the marine shrimp *Sicyonia ingentis. Dev. Biol.* **152,** 94–102.

Miyazaki, S. (1995). Calcium signaling during mammalian fertilization. *In* "Calcium Waves, Gradients and Oscillations" (G. R. Bock and K. Ackrill, Eds.), Ciba Foundation Symposium, Vol. 188, pp. 235–247. Wiley, Chichester, UK.

Miyazaki, S., Hashimoto, N., Yoshimoto, Y., Kishimoto, T., Igusa, Y., and Hiramoto, Y. (1986). Temporal and spatial dynamics of the periodic increase in intracellular free calcium at fertilization of golden hamster eggs. *Dev. Biol.* **118,** 259–267.

Miyazaki, S., and Hirai, S. (1979). Fast polyspermy block and activation potential. Correlated changes during oocyte maturation of a starfish. *Dev. Biol.* **70,** 327–340.

Miyazaki, S., Shirakawa, H., Nakada, K., and Honda, Y. (1993). Essential role of the inositol 1,4,5-trisphosphate receptor/Ca^{2+} release channel in Ca^{2+} waves and Ca^{2+} oscillations at fertilization of mammalian eggs. *Dev. Biol.* **158,** 62–78.

Nuccitelli, R. (1980). The fertilization potential is not necessary for the block to polyspermy or the activation of development in the medaka egg. *Dev. Biol.* **76,** 499–504.

Parrington, J., Swann, K., Shevchenko, V. I., Sesay, A. K., and Lai, F. A. (1996). Calcium oscillations in mammalian eggs triggered by a soluble sperm protein. *Nature* **379,** 364–368.

Pillai, M. C., and Clark, W. H., Jr. (1987). Oocyte activation in the marine shrimp, *Sicyonia ingentis. J. Exp. Zool.* **244,** 325–329.

Roberts, S. K., Gillot, I., and Brownlee, C. (1994). Cytoplasmic calcium and *Fucus* egg activation. *Development* **120,** 155–163.

Roosen-Runge, E. C. (1938). On the early development—bipolar differentiation and cleavage—of the zebrafish, *Brachydanio rerio. Biol. Bull.* **75,** 119–133.

Rothschild, Lord (1958). Fertilization in fish and lampreys. *Biol. Rev. Camb. Philos. Soc.* **33,** 372–392.

Sakai, N., Burgess, S., and Hopkins, N. (1997). Delayed *in vitro* fertilization of zebrafish eggs in Hank's saline containing bovine serum albumin. *Mol. Mar. Biol. Biotech.* **6,** 84–87.

Schalkoff, M. E., and Hart, N. H. (1986). Effects of A23187 upon cortical granule exocytosis in eggs of *Brachydanio. Roux's Arch. Dev. Biol.* **195,** 39–48.

Shen, S. S. (1995). Mechanisms of calcium regulation in sea urchin eggs and their activities during fertilization. *Curr. Top. Dev. Biol.* **30,** 63–101.

Shimomura, O. (1995). Luminescence of aequorin is triggered by the binding of two calcium ions. *Biochem. Biophys. Res. Commun.* **211,** 359–363.

Shimomura, O., Inouye, S., Musicki, B., and Kishi, Y. (1990). Recombinant aequorins and recombinant semi-synthetic aequorins. *Biochem. J.* **270,** 309–312.

Smith, J. D., Dwyer, S. D., and Smith, L. (1989). Cadmium evokes inositol polyphosphate formation and calcium mobilization. Evidence for a cell surface receptor that cadmium stimulates and zinc antagonizes. *J. Biol. Chem.* **264,** 7115–7118.

Speksnijder, J. E., Sardet, C., and Jaffe, L. F. (1990). Periodic calcium waves cross ascidian eggs after fertilization. *Dev. Biol.* **142,** 246–249.

Stephano, J. L., and Gould, M. C. (1997). The intracellular calcium increase at fertilization in *Urechis caupo* oocytes: Activation without waves. *Dev. Biol.* **191,** 53–68.

Steinhardt, R., Zucker, R., and Schatten, G. (1977). Intracellular calcium release at fertilization in the sea urchin egg. *Dev. Biol.* **58,** 185–196.

Stricker, S. A. (1996). Repetitive calcium waves induced by fertilization in the nemertean worm *Cerebratulus lacteus. Dev. Biol.* **176,** 243–263.

Stricker, S. A., Centonze, V. E., Paddock, S. W., and Schatten, G. (1992). Confocal microscopy of fertilization-induced calcium dynamics in sea urchin eggs. *Dev. Biol.* **149,** 370–380.

Swann, K. (1993). The soluble sperm oscillogen hypothesis. *Zygote* **1,** 273–276.

Swann, K. (1994). Ca^{2+} oscillations and sensitization of Ca^{2+} release in unfertilized mouse eggs injected with a sperm factor. *Cell Calcium* **15,** 331–339.

Swann, K., and Lai, F. A. (1997). A novel signaling mechanism for generating Ca^{2+} oscillations at fertilization in mammals. *BioEssays* **19,** 371–378.

Tesarik, J., and Testart, J. (1994). Treatment of sperm-injected human oocytes with Ca^{2+} ionophore supports the development of Ca^{2+} oscillations. *Biol. Reprod.* **51,** 385–391.

Webb, S. E., Lee, K. W., Karplus, E., and Miller, A. L. (1997). Localized calcium transients accompanying furrow positioning, propagation, and deepening during the early cleavage period of zebrafish embryos. *Dev. Biol.* **192,** 78–92.

Westerfield, M. (1994). "The Zebrafish Book: A Guide for the Laboratory Use of Zebrafish (*Brachydanio rerio*)." Univ. of Oregon Press, Eugene, OR.

Whitaker, M., and Swann, K. (1993). Lighting the fuse at fertilization. *Development* **117,** 1–12.

Wolenski, J. S., and Hart, N. H. (1987). Scanning electron microscope studies of sperm incorporation into the zebrafish (*Brachydanio*) egg. *J. Exp. Zool.* **243,** 259–273.

Yamamoto, T. (1944). Physiological studies on fertilization and activation of fish eggs. II. The conduction of the "fertilization-wave" in the egg of *Oryzias latipes. Annot. Zool. Jpn.* **22,** 126–136.

Yamamoto, T. (1954). Cortical changes in eggs of the goldfish (*Carassius auratus*) and the pond smelt (*Hypomesus olidus*) at the time of fertilization and activation. *Jpn. J. Ichthyol.* **3,** 162–170.

Yamamoto, T. (1961). Physiology of fertilization in fish eggs. *Int. Rev. Cyt.* **12,** 361–405.

Yoshimoto, Y., Iwamatsu, T., Hirano, K., and Hiramoto, Y. (1986). The wave pattern of free calcium release upon fertilization in medaka and sand dollar eggs. *Dev. Growth Differ.* **28,** 583–596.

Received for publication April 20, 1999
Accepted July 6, 1999